NEW I/Q IMBALANCE MODELING AND COMPENSATION IN OFDM SYSTEMS WITH FREQUENCY OFFSET

Sébastien Simoens, Marc de Courville, François Bourzeix†, Paul de Champs†

Motorola Labs Paris
Espace Technologique de St-Aubin
91193 Gif-sur-Yvette Cedex FRANCE
†Motorola Semiconductors Geneva
E-mail: simoens@motorola.com

ABSTRACT

In this paper, a new model and compensation scheme of quadrature imbalance in analog I/Q OFDM transceivers is presented. Classically, the effect of I/Q imbalance is modeled by a cross-talk between pairs of symmetrical OFDM sub-carriers. We show that this model is not valid when the carrier frequency offset is compensated after the source of I/Q mismatch. Assuming a perfect digital compensation of the frequency offset in baseband, the I/Q imbalance generates interference between all sub-carriers and not only symmetrical ones. When analog components, multipath propagation and frequency offsets are taken into account, the complete matrix analysis has to make use of mathematical results such as the diagonalization of pseudo-circulant matrices. The existing models happen to be a sub-case of this new more general result. A new compensation scheme applying to every case is proposed as well as a receiver auto-calibration procedure. It is shown that system-specific assumptions can simplify the implementation of the compensation. These assumptions are validated by simulation in the framework of a 5GHz WLAN transceiver design with realistic production spread of the analog components.

1. INTRODUCTION

Orthogonal Frequency Division Multiplexing (OFDM) [1] systems are widespread in broadcasting (DAB,DVB-T) and new wireless LAN standards [2] (IEEE802.11a and g, HIPERLAN/2). In terms of RF architecture, analog I/Q transceivers have been and remain widely used in digital communication systems. This type of architecture includes heterodyne receivers with one or several intermediate frequencies (IF) and also the more recent direct-conversion receivers [3]. A limitation of analog I/Q is the presence of quadrature imbalance between the I and Q paths of the transmitter and/or the receiver. The mixers gain and phase imbalance is generally constant over the OFDM signal bandwidth, whereas channel-selection or anti-aliasing filtering imbalance, A/D gain and clock imbalance are likely to exhibit faster variations.

Digital I/Q generation [4] is an alternative that has the advantage, among others, of inherently avoiding I/Q imbalance but requires a higher sampling rate (at least twice that of analog I/Q) and the digital filtering of I and Q signals. For wideband signals like IEEE802.11a [2] having a 20 MHz bandwidth and 60 GHz systems [5] with a bandwidth larger than 100 MHz, it can be preferred in terms of circuit area and power consumption to keep an analog I/Q architecture. However high order modulations like 64 QAM might then put too stringent constraints on the analog design. Several digital imbalance compensation techniques have been proposed [6, 7], aiming at a solution that would combine the low hardware complexity and power consumption of analog I/Q with the signal quality of digital I/Q.

In [8] and [9], it is shown that I/Q imbalance (a.k.a. I/Q mismatch) produces cross-talk between symmetrical sub-carriers of OFDM signal. Based on this model, a compensation scheme of frequency-dependent I/Q imbalance for OFDM systems is proposed in [6]. However, these models and the associated compensation schemes prove to be incorrect when a carrier frequency offset occurring in the down-conversion is compensated digitally in baseband. In [10], it is shown that carrier frequency offset gives rise to Inter Carrier Interference (ICI) in the frequency domain (after the Discrete Fourier Transform (DFT)) and must be accurately compensated before the DFT. In section 2, we derive the effect of I/Q imbalance on the frequency-domain signal assuming perfect digital compensation of the carrier frequency offset in baseband. The necessary matrix computations are summarized in the annex. This model shows that the I/Q mismatch produces ICI involving every sub-carrier and not only symmetrical ones. In section 3, a frequency domain estimation and compensation algorithm is proposed with several approximations enabling simple implementa-

0-7803-7589-0/02/$17.00

tion. Finally, in section 4, simulations of a 5 GHz OFDM Wireless LAN transceiver illustrate an application of the estimation and compensation scheme.

2. MODELING OF I/Q IMBALANCE WITH FREQUENCY OFFSETS

In this section, the model of the OFDM transmission is presented and the effect of I/Q imbalance on the frequency-domain signal, derived in the annex, is provided. The calculations are based on the notations of fig. 4, which models an OFDM transmission with balanced I/Q at the transmitter, I/Q imbalance at the receiver and carrier frequency offset. For simplicity, noise is not represented and the transmit I/Q imbalance is not included. But results will be given for both transmit and receive I/Q imbalance. We use the following conventions: $\mathbf{v}$ is a vector , $\mathbf{V}$ is a matrix and v_i denotes the ith component of $\mathbf{v}$. $\tilde{v}$ is a time-domain vector. The operator * denotes the component-wise complex conjugation. The N components of frequency domain OFDM symbol $\mathbf{d} = (d_{-\frac{N}{2}}, d_{-\frac{N}{2}+1}, ..., d_{\frac{N}{2}-1})^t$ are modulated by the IDFT. Then a cyclic extension of length E samples is inserted. The complex samples are denoted $\tilde{\mathbf{d}} = (\tilde{d}_{-E}, \tilde{d}_{-E+1}, ..., \tilde{d}_{N-1})$. The duration of an OFDM symbol is $(N+E)T$, where T is the sampling period. After D/A conversion and low-pass filtering, the I and Q signals modulate an IF carrier, or directly the RF carrier in a zero-IF architecture. The IDFT inputs corresponding to DC and sub-carriers at the edges of the signal spectrum are actually set to zero, which is not represented here for simplicity. This facilitates D/A conversion and low-pass filtering which effectively limit the bandwidth to $\frac{1}{T}$. Here the effects of the whole analog transmitter combined with the propagation channel are summarized by the discrete filtering of $\tilde{\mathbf{d}}$ by $\tilde{\mathbf{h}}$. The receiver introduces carrier frequency offset $\frac{\varepsilon}{T}$ during down-conversion and I/Q imbalance. The ratio between the quadrature and the in-phase mixers gain is β and their phase difference equals ϕ. The cross-talk between I and Q signals due to mixers imbalance is well-known [8]. The other sources of imbalance are gathered in filters of impulse response $\tilde{\mathbf{g}}_I$ and $\tilde{\mathbf{g}}_Q$. In the digital part of the receiver, it is assumed that a perfect carrier frequency compensation is applied to $\tilde{\mathbf{p}}$. Samples corresponding to the cyclic extension are removed and frequency-compensated vector $\tilde{\mathbf{r}}$ of size N is demodulated by the DFT producing $\mathbf{r}$. We make the well-known assumption that the overall convolution of transmit, propagation and any of the two receive filters remains shorter than the cyclic extension. As a consequence, there is no Inter Block Interference between successive OFDM symbols and the calculus is performed on a single OFDM symbol during which $\tilde{\mathbf{h}}$ is assumed constant. The terms involving the previous OFDM symbol are systematically removed from the equations of the annex, with no impact on the final result. In the annex, the expression of $\mathbf{r}$ as a function of $\mathbf{d}$ is derived by block matrix calculations and diagonalization of pseudo-circulant matrices, leading to:

$$\mathbf{r} = \mathbf{r}^+ + \mathbf{r}^- \tag{1}$$

of components:

$$r_i^+ = h_i g_i^+(\varepsilon) d_i \tag{2}$$

$$r_i^- = \sum_{k=-\frac{N}{2}}^{\frac{N}{2}-1} \lambda_{k-i} g_k^-(-\varepsilon) h_{-k}^\star d_{-k}^\star \tag{3}$$

where:

- $$\lambda_i = \frac{1}{N} \exp\left[j\pi(N-1)\left(\frac{i}{N} - 2\varepsilon\right)\right] \frac{\sin\left[\pi N\left(\frac{i}{N} - 2\varepsilon\right)\right]}{\sin\left[\pi\left(\frac{i}{N} - 2\varepsilon\right)\right]} \tag{4}$$
- $h_k = \sum_{i=0}^{N-1} \tilde{h}_i e^{-j2\pi\frac{ik}{N}}$ is the kth channel frequency coefficient
- $g_k^+(\varepsilon)$ (resp. $g_k^-(-\varepsilon)$) is the z-transform of $\mathbf{g}^+$ (resp. $\mathbf{g}^-$) evaluated at point $e^{j2\pi\left(\frac{k}{N}+\varepsilon\right)}$ (resp. $e^{j2\pi\left(\frac{k}{N}-\varepsilon\right)}$).
- $\mathbf{g}^+$ and $\mathbf{g}^-$ are defined by $\mathbf{g}^+ = \frac{\tilde{\mathbf{g}}_I + \beta e^{-j\phi}\tilde{\mathbf{g}}_Q}{2}$ and $\mathbf{g}^- = \frac{\tilde{\mathbf{g}}_I - \beta e^{j\phi}\tilde{\mathbf{g}}_Q}{2}$. Obviously, when there is no I/Q imbalance, $\tilde{\mathbf{g}}^+ = \tilde{\mathbf{g}}_I = \tilde{\mathbf{g}}_Q$ and $\tilde{\mathbf{g}}^- = \mathbf{0}$.

These equations deserve a few comments:

- r_i^+ can be viewed as the useful part of r_i: the transmitted symbol is multiplied by the channel and by the receive filter frequency response evaluated at the sub-carrier frequency (which is shifted by ε because frequency compensation is applied after the reception filter
- r_i^- corresponds to ICI. When the carrier frequency offset is negligible or is perfectly compensated before the I and Q filters, then $\lambda_i = \begin{cases} 1 & \text{if } i = 0 \\ 0 & \text{else} \end{cases}$ and the ICI reduces to the well-known [8, 9] cross-talk between symmetrical sub-carriers i and $-i$
- The problem is that crystals used to generate the down-conversion frequencies by PLL synthesizers typically have a stability of several ppm. For instance in HIPERLAN/2 and 802.11a, the tolerated frequency offset between transmitter and receiver is 40 ppm. It can be verified that with 40 ppm (and even with 5 ppm) the $\lambda_{i,i\neq 0}$ are not negligible. Besides, accurately controlling the

oscillator (e.g. using a VCXO) is not easy, therefore it can be preferred to compensate the frequency offset by digital signal processing means in the baseband as illustrated on figure 4

- Notice that the calculus for transmit I/Q imbalance would be simpler since there is no digital baseband pre-compensation of the frequency offset at the transmitter side, and would lead to cross-talk between pairs of symmetrical sub-carriersat the input of the IDFT.

To summarize, I/Q imbalance produces ICI when frequency offset is compensated (even perfectly) just before the DFT. How to compensate this ICI with minimum complexity is addressed in the next section.

3. ESTIMATION AND COMPENSATION OF THE IMBALANCE

As shown in equations (2) and (3) of the previous section the frequency offset, although perfectly corrected, makes I/Q imbalance compensation in the frequency domain a difficult task since the interference on a sub-carrier results from the contribution of all sub-carriers. Fortunately, two approximations can be performed which simplify the equations and enable a low-complexity implementation of the compensation. These approximations are verified in the specific context of a 5 GHz WLAN transceiver in section 4.

The first simplification is obtained by assuming that the ICI is small compared to the signal power, i.e. $|r_i^-| \ll |r_i^+|$ $\forall i$. Rewriting (1) as:

$$r_i = r_i^+ + \sum_{k=-\frac{N}{2}}^{\frac{N}{2}-1} \lambda_{k-i}\alpha_k {r_{-k}^+}^\star \quad (5)$$

with $\alpha_k \hat{=} \dfrac{g_k^-(-\varepsilon)}{g_{-k}^+(+\varepsilon)^\star}$ and applying the approximation to (5) yields:

$$r_i^+ \approx r_i - \sum_{k=-\frac{N}{2}}^{\frac{N}{2}-1} \lambda_{k-i}\alpha_k r_{-k}^\star \quad (6)$$

The second simplification comes from the observation that $\left|\dfrac{\sin(\pi N x)}{\sin(\pi x)}\right|$ drops when $|x|$ increases. Therefore, the compensated sub-carrier $\hat{r}_i^+$ can be obtained from the DFT output r_i as follows:

$$\boxed{\hat{r}_i^+ = r_i - \sum_{\substack{-\frac{N}{2} \leq k \leq \frac{N}{2}-1 \\ |k-i-N\varepsilon|<K_{max}}} \lambda_{k-i}\alpha_k r_{-k}^\star} \quad (7)$$

The $\hat{r}_i^+$ will then be phase compensated and equalized by classical means, which is out of the scope of this paper. In the implementation of the compensation, the λ_i can be pre-computed given the frequency offset estimate. The constant K_{max} is typically small as shown in section 4 (e.g. $K_{max} = 2$) and determines the number of FFT outputs involved in the recombination. Notice that, very similarly, compensating transmit I/Q imbalance would require the combination of IDFT inputs corresponding to opposite sub-carrier frequencies. Anyway, the coefficients α_k have to be estimated prior to transmission and this estimation is the purpose of the next paragraph.

In order to estimate the α_k coefficients, a simple solution is to send a pilot signal and avoid the presence of a carrier frequency offset. The pilot signal has to cross the various parts of the transceiver which potentially contribute to the I/Q imbalance. Among the various possible implementations, we focus on the one described on figure 1, which is suited to transceivers in which the imbalance only comes from the low-pass filters. A very simple OFDM pilot signal is generated by the DSP unit. The simplest one is defined by:

$$d_i = \begin{cases} 1 & 1 \leq i \leq \frac{N}{2} \\ 0 & \text{otherwise} \end{cases} \quad (8)$$

After D/A conversion, the I and Q paths are not routed to the up-conversion stage of the RF transceiver but to the reception I and Q filters by two switches. The received OFDM signal is such that:

$$r_i = \alpha_i r_{-i}^\star \quad , -\tfrac{N}{2} \leq i \leq -1 \quad (9)$$

$\alpha(i)$ is thus estimated from r_i as follows:

$$\alpha(i) = \frac{r_i}{r_{-i}^\star} \quad -\tfrac{N}{2} \leq i \leq -1 \quad (10)$$

$$\alpha(i) = \alpha^\star(-i) \quad 1 \leq i \leq \tfrac{N}{2} \quad (11)$$

Equation (11) comes from the fact that $\tilde{\mathbf{g}}_I$ and $\tilde{\mathbf{g}}_Q$ are real vectors and therefore their frequency response has Hermitian symmetry. This scheme is very simple but neglects the dependence of $\alpha(i)$ on ε. The validity of this assumption depends of course on the value of the frequency offset and on the filters frequency response. An example of application of the training procedure is given in section 4. I/Q imbalance is mainly due to production spread and in smaller proportions to thermal effects. Therefore this sort of calibration procedure does not have to be executed frequently. If there is I/Q imbalance in the mixers, then a test tone [7] could be generated at each sub-carrier frequency.

In this section, a compensation scheme has been proposed along with an estimation procedure. Several approximations have been necessary to simplify both compensation and estimation. In the following section, we simulate them with real product data in order to assess the validity of the assumptions.

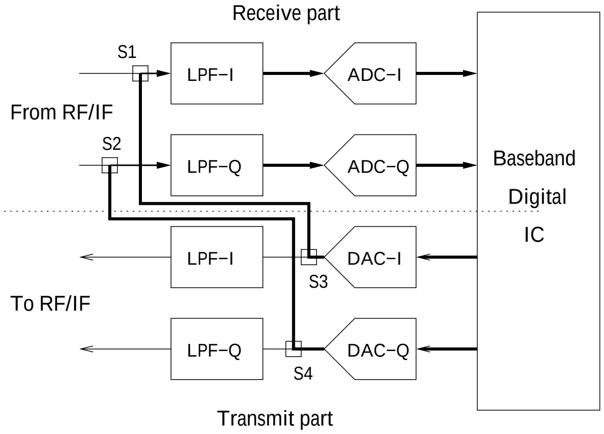

Figure 1: Example of hardware configuration for receiver I/Q imbalance estimation

4. SIMULATION RESULTS

As stated before, the estimation and compensation procedures presented in the previous section rely on several approximations which need validation with actual value. In this section, we apply both methods to an OFDM transceiver where the imbalance comes from a 7^{th} order Chebyshev low-pass filter (LPF) which is the channel selection and anti-aliasing filter of a IEEE802.11a or HIPERLAN/2 analog I/Q transceiver. Production spread of the components was simulated under SPICE^{TM}. The edge sub-carriers of these 5 GHz systems are at +/- 8.125 MHz from the center frequency. On figure 2, the gain and phase mismatch of the LPFs frequency response is represented. The mismatch increases when approaching the corner frequency. According to [8], a gain imbalance of $G_{\text{imb}} = 0.7$ dB produces a Signal to Interference Ratio (SIR) of

$$SIR(G_{\text{imb}}) = 20 \ \log \ \frac{1}{\left|\frac{10^{G_{\text{imb}}/20}-1}{10^{G_{\text{imb}}/20}+1}\right|} = 27.9dB$$

and a phase imbalance of $\phi_{\text{imb}} = 10°$ results in

$$SIR(\phi_{\text{imb}}) = 20 \log\left(\text{cotan}\frac{\phi_{\text{imb}}}{2}\right) = 21.1dB$$

Actually the imbalance depends on frequency, but the figures above give an idea of the level of degradation expected, and validate the small-imbalance assumption performed in section 3. On figure 3, the Packet Error Rate (PER) performance of the 54 Mbit/s mode (64QAM rate 3/4) mode of HIPERLAN/2 was simulated in a typical office environment. Transmit and receive filters are the same and undergo the same mismatch. The 200 kHz carrier frequency offset is perfectly compensated just before the FFT. The degradation due to I/Q imbalance reaches 5dB at PER=3% (dotted curve). Applying only transmit pre-compensation improves the performance and when both transmit and receive compensation are applied, the degradation reduces to 1dB at PER=1% (dashed curves). This 1dB results from several effects:

- Only 2 coefficients were used in the receiver compensation to have low complexity.
- The calibration procedure in the receiver neglected the frequency offset.
- The filters with and without production spread are slightly different anyway, especially their impulse response duration which, combined with channel multipath, has an impact on the performance.

5. CONCLUSION

A novel I/Q imbalance model in OFDM systems was presented. Considering the interaction of I/Q imbalance with carrier frequency offset in a multipath propagation environment, the effect on the received signal was derived by complex matrix calculations. A new compensation scheme was then proposed, and a simple implementation was derived using system-specific assumptions. A mismatch estimation procedure was also proposed in order to set the parameters of the compensation algorithm. Finally, both procedures and assumptions were illustrated in the framework of a WLAN transceiver design with realistic specifications.

Acknowledgements

The authors would like to thank David Bateman and Markus Muck from Motorola Labs Paris, as well as Anil Gercekci, Heinz Lehning and Thien Huynh from SPS Geneva for their technical advise and support.

6. REFERENCES

[1] B. Le Floch, M. Alard, and C. Berrou. Coded orthogonal frequency division multiplex (TV broadcasting). *Proceedings of the IEEE*, 83(6):982–996, June 1995.

[2] R. Van Nee et al. New high-rate wireless LAN standards. *IEEE Communications Magazine*, 40:140–147, January 2002.

[3] B. Razavi. Design Considerations for Direct-Conversion Receivers. *IEEE Transactions on Circuits and Systems*, 44:428–435, June 1997.

[4] W.M. Waters and B. R. Jarrett. Bandpass Signal Sampling and coherent detection. *IEEE Trans. on Aerospace and Electronic Systems*, 18:731–736, November 1998.

[5] Peter Smulders. Exploiting the 60 GHz band for local multimedia access: prospects and future directions. *IEEE Trans. on Communications*, 37:82–88, December 1999.

[6] A. Schuchert, R. Hasholzner, and P. Antoine. A novel IQ imbalance compensation scheme for the reception of OFDM signals . *IEEE Trans. on Consumer Electronics*, 47:313–318, August 2001.

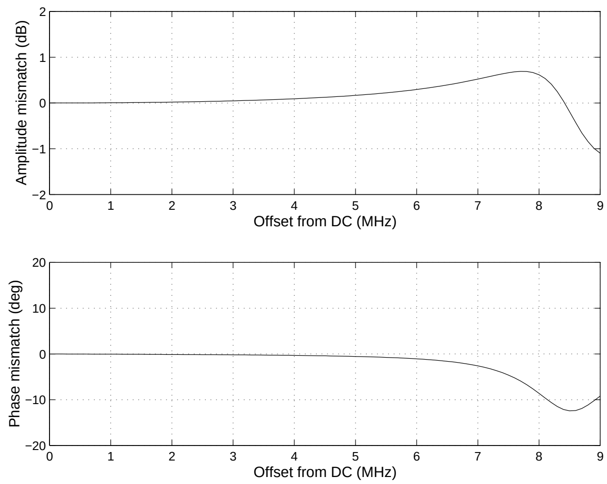

Figure 2: Worst case mismatch of the baseband LPFs

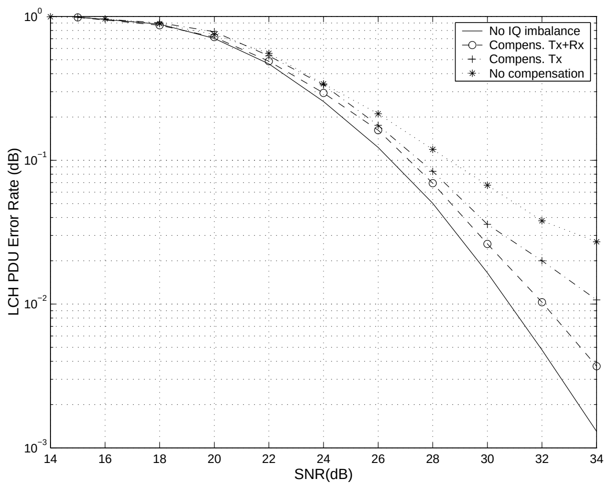

Figure 3: Impact of I/Q imbalance compensation on PER performance (64QAM,R=3/4)

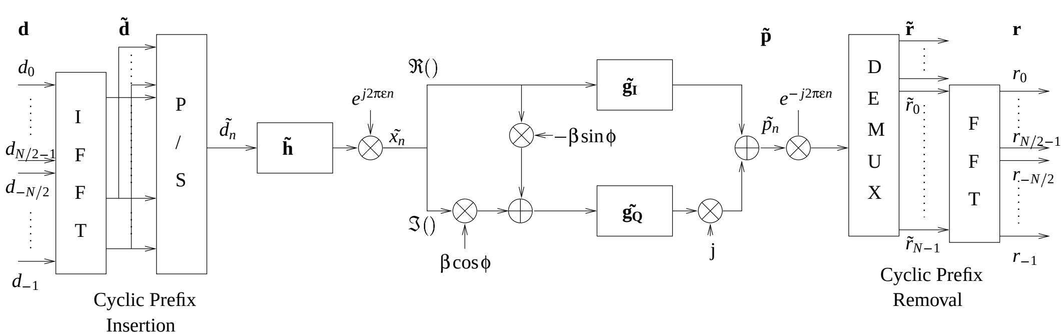

Figure 4: Model of OFDM transmission with frequency offset and receiver I/Q imbalance

[7] J.P.F Glas. Digital I/Q imbalance compensation in a low-IF receiver. In *GLOBECOM conference records*, volume 3, pages 1461–1466, 1998.

[8] C-L. Liu. Impacts of I/Q imbalance on QPSK-OFDM-QAM detection. *IEEE Trans. on Consumer Electronics*, 44:984–989, August 1998.

[9] M-G. Di Benedetto and P. Mandarini. Analysis of the effect of the I/Q Base-Band Filter Mismatch in an OFDM Modem. *Wireless Personal Communications*, pages 175–186, February 2000.

[10] T. Pollet, M. van Bladel, and M. Moeneclaey. BER sensitivity of OFDM systems to carrier frequency offset and Wiener phase noise. *IEEE Trans. on Communications*, 43:191–193, February 1995.

Appendix

This annex aims at summarizing the theoretical justification of the frequency modeling of the I/Q mismatch expression of equations (2) and (3).

Denote by $\mathbf{M}_{\text{CP}}$ and $\mathbf{S}_{\text{CP}}$ the operators for cyclic prefix insertion at the transmitter and removal at the receiver: $\mathbf{M}_{\text{CP}} \hat{=} \left[\begin{array}{c|c} \mathbf{0}_{E,N-E} & \mathbf{I}_E \\ \hline \multicolumn{2}{c}{\mathbf{I}_N} \end{array}\right]$, $\mathbf{S}_{\text{CP}} \hat{=} \left[\begin{array}{c|c} \mathbf{0}_{N,E} & \mathbf{I}_N \end{array}\right]$. The following lower left and upper right Toeplitz matrices of size $l \times l$ are also defined:

$$\mathbf{G}_L(l) = \begin{bmatrix} \tilde{g}_0 & 0 & \rightarrow & 0 \\ \tilde{g}_1 & \searrow & \searrow & \downarrow \\ \vdots & \searrow & \searrow & 0 \\ \tilde{g}_{l-1} & \cdots & \tilde{g}_1 & \tilde{g}_0 \end{bmatrix}$$

$$\mathbf{G}_U(l) = \begin{bmatrix} 0 & \tilde{g}_{l-1} & \cdots & \tilde{g}_1 \\ \downarrow & \searrow & \searrow & \vdots \\ \downarrow & & \searrow & \tilde{g}_{l-1} \\ 0 & \rightarrow & \rightarrow & 0 \end{bmatrix}$$

With these notations, $\mathbf{H}_L(N+E)$ represents the filtering by channel $\tilde{\mathbf{h}}$, $\mathbf{G}_L^+(N+E)$ (resp. $\mathbf{G}_L^-(N+E)$) the filtering by $\mathbf{g}^+$ (resp. $\mathbf{g}^-$). Notice that the impulse response of these filters is shorter than E so many diagonals are actually zero.

The carrier frequency offset corresponds to a multiplication by the following matrix:

$$\mathbf{D} \hat{=} \operatorname{diag}\left(e^{-j2\pi E\varepsilon}, \cdots, 1, e^{j2\pi N\varepsilon}, \cdots, e^{j2\pi(N-1)\varepsilon}\right)$$

We introduce a block notation for $\mathbf{D}$ to separate the cyclic prefix from the rest of the symbol: $\mathbf{D} \hat{=} \left[\begin{array}{c|c} e^{-j2\pi N\varepsilon}\mathbf{D}_0 & \mathbf{0}_{E,N} \\ \hline \mathbf{0}_{N,E} & \mathbf{D}_1 \end{array}\right]$ with $\mathbf{D}_1 \hat{=} \left[\begin{array}{c|c} \mathbf{D}_2 & \mathbf{0}_{N-E,E} \\ \hline \mathbf{0}_{E,N-E} & \mathbf{D}_0 \end{array}\right]$ The frequency offset correction consists in multiplying the useful samples by $\mathbf{D}_1^\star$. With these notations, it is possible to express $\mathbf{r}^+$ and $\mathbf{r}^-$ as:

$$\mathbf{r}^+ = \mathbf{F}\mathbf{D}_1^\star \mathbf{S}_{\text{CP}} \mathbf{G}_L^+(N+E)\mathbf{D}\mathbf{H}_L(N+E)\mathbf{M}_{\text{CP}}\mathbf{F}^{-1}\mathbf{d} \quad (12)$$

$$\mathbf{r}^- = \mathbf{F}\mathbf{D}_1^\star \mathbf{S}_{\text{CP}} \mathbf{G}_L^-(N+E)\mathbf{D}^\star\mathbf{H}_L^\star(N+E)\mathbf{M}_{\text{CP}}(\mathbf{F}^{-1}\mathbf{d})^\star \quad (13)$$

Where $\mathbf{F}$ is the DFT matrix of size N: $F_{i,j} = \frac{1}{\sqrt{N}} e^{-j2\pi\frac{ij}{N}}$. Focusing at first on (12), we introduce the following decomposition of the identity matrix between $\mathbf{D}$ and $\mathbf{H}_L(N+E)$:

$$\mathbf{M}_{\text{CP}}\mathbf{F}^{-1}\mathbf{F}\mathbf{S}_{\text{CP}} + \left[\begin{array}{c|c|c} \mathbf{I}_{E,E} & \mathbf{0}_{E,N-E} & -\mathbf{I}_{E,E} \\ \hline \multicolumn{3}{c}{\mathbf{0}_{N,P}} \end{array}\right] \quad (14)$$

This trick enables us to introduce artificially the cyclic prefix insertion and removal operators between the Toeplitz matrices $\mathbf{G}_L^+(N+E)$ and $\mathbf{H}_L(N+E)$. It can be checked that the left hand term of (14) cancels out during calculation under the assumption that the sum of the lengths of the impulse responses of the filters is shorter than the cyclic prefix. The following two properties are then used to diagonalize the Toeplitz matrices:

1. A circulant matrix is diagonalized in the Fourier basis.Therefore,

$$\mathbf{F}\mathbf{S}_{\text{CP}}\mathbf{H}_L(N+E)\mathbf{M}_{\text{CP}}\mathbf{F}^{-1} = \mathbf{F}\underbrace{(\mathbf{H}_L(N)+\mathbf{H}_U(N))}_{\text{circulant}}\mathbf{F}^{-1} \quad (15)$$
$$= \operatorname{diag}(\sqrt{N}\mathbf{F}\tilde{\mathbf{h}}) \quad (16)$$

2. a more general (yet less known) result applies to pseudo-circulant matrices such as $\mathbf{G}_L^+(N) + e^{-j2\pi\varepsilon N}\mathbf{G}_U^+(N)$:

$$\begin{aligned} & \mathbf{F}\mathbf{D}_1^\star\mathbf{S}_{\text{CP}}\mathbf{G}_L^+(N+E)\mathbf{D}\mathbf{M}_{\text{CP}}\mathbf{F}^{-1} \\ = \; & \mathbf{F}\mathbf{D}_1^\star(\mathbf{G}_L^+(N)+e^{-j2\pi\varepsilon N}\mathbf{G}_U^+(N))\mathbf{D}_1\mathbf{F}^{-1} \\ = \; & \operatorname{diag}(\mathbf{g}_\varepsilon^+) \end{aligned} \quad (17)$$

Finally, reintroducing (16) and (17) into (12) yields expression (2) of section 2.

The same calculus holds for the expression of $\mathbf{d}^-$ leading to:

$$\mathbf{r}^- = \underbrace{\mathbf{F}\mathbf{D}_1^\star\mathbf{D}_1^\star\mathbf{F}^{-1}}_{\text{Circulant Matrix}} \operatorname{diag}(\mathbf{g}_{-\varepsilon}^-)\operatorname{diag}(\mathbf{S}(\sqrt{N}\mathbf{F}\tilde{\mathbf{h}})^\star)\mathbf{S}\mathbf{d}^\star \quad (18)$$
$$= \operatorname{circ}(\lambda)\operatorname{diag}(\mathbf{g}_{-\varepsilon}^-)\operatorname{diag}(\mathbf{S}(\sqrt{N}\mathbf{F}\tilde{\mathbf{h}})^\star)\mathbf{S}\mathbf{d}^\star \quad (19)$$

Where it can be checked that $\mathbf{S} \hat{=} \mathbf{F}\mathbf{F}$ is a permutation matrix which exchanges symmetrical sub-carriers, and $\operatorname{circ}(\lambda)$ is the circulant matrix of which the first line is $\lambda = (\lambda_0, \lambda_1, \ldots, \lambda_{N-1})$ as defined in (4).